NASA CR-160030

HIGH RESOLUTION INFRARED RADIATION SOUNDER/MOD 2 (HIRS/2)

FINAL PROJECT REPORT

CONTRACT NAS5-23567

Prepared For:

National Aeronautics and Space Administration
Goddard Space Flight Center
Greenbelt, Maryland 20771

Prepared By:

ITT Aerospace Optical Division
3700 East Pontiac Street
Fort Wayne, Indiana 46803

August 1979

UNCLASSIFIED

SECURITY CLASSIFICATION OF THIS PAGE (When Data Entered)

REPORT DOCUMENTATION PAGE

READ INSTRUCTIONS BEFORE COMPLETING FORM

1. REPORT NUMBER	2. GOVT ACCESSION NO. / 3. RECIPIENT'S CATALOG NUMBER
4. TITLE (and Subtitle): FINAL REPORT ON THE HIGH RESOLUTION INFRARED RADIATION SOUNDER/MOD 2 (HIRS/2)	5. TYPE OF REPORT & PERIOD COVERED: Final, 1976 to 1979
	6. PERFORMING ORG. REPORT NUMBER
7. AUTHOR(s): Edward W. Koenig, et. al.	8. CONTRACT OR GRANT NUMBER(s): NAS5-23567
9. PERFORMING ORGANIZATION NAME AND ADDRESS: ITT Aerospace/Optical Division, 3700 E. Pontiac Street, Fort Wayne, Indiana 46803	10. PROGRAM ELEMENT, PROJECT, TASK AREA & WORK UNIT NUMBERS
11. CONTROLLING OFFICE NAME AND ADDRESS: National Aeronautics & Space Administration, Goddard Space Flight Center, Greenbelt, Maryland 20771	12. REPORT DATE: August 1979 / 13. NUMBER OF PAGES
14. MONITORING AGENCY NAME & ADDRESS(if different from Controlling Office)	15. SECURITY CLASS. (of this report): Unclassified / 15a. DECLASSIFICATION/DOWNGRADING SCHEDULE

16. DISTRIBUTION STATEMENT (of this Report)

GSFC Publication Branch Code 251
GSFC Technical Officer Code Code 480

17. DISTRIBUTION STATEMENT (of the abstract entered in Block 20, if different from Report)

18. SUPPLEMENTARY NOTES

19. KEY WORDS (Continue on reverse side if necessary and identify by block number)

Atmosphere Sounding
Radiometer
Temperature Profile
Radiative Cooling

20. ABSTRACT (Continue on reverse side if necessary and identify by block number)

The HIRS/2 is provided for the TIROS-N series of operational meteorological satellites. Instrument features 20 spectral channels, including visible (.7 micron), shortwave (3.7 to 4.6 micron) and longwave (6.7 to 15 micron). Radiance data aids determination of vertical temperature profiles, water vapor and ozone distribution. This report describes system performance and test results.

DD FORM 1 JAN 73 1473 EDITION OF 1 NOV 65 IS OBSOLETE

UNCLASSIFIED

SECURITY CLASSIFICATION OF THIS PAGE (When Data Entered)

Table of Contents

List of Figures

List of Tables

PREFACE

The High Resolution Infrared Radiation Sounder (HIRS/2) program provides operational instrumentation for the collection of atmospheric radiance data that will permit calculation of temperature profile from the surface to 10 mb, water vapor content in three layers of the atmosphere, and total ozone content. Radiance is measured in nineteen selected infrared channels. One visible channel senses solar reflectance to aid albedo and cloud cover determination. Cross-track scanning provides near full earth coverage twice each day.

Three instruments developed and fabricated on this contract are for use on the TIROS-N satellite series. The first unit was a part of the TIROS-N satellite launched on October 13, 1978. Data from the first instrument became operational on March 1, 1979. The second unit was a part of the NOAA-6 satellite launched on June 27, 1979. The third unit has been delivered to the spacecraft integrator for assembly into the NOAA-B spacecraft.

This report describes the instrument, its program history, and the more significant test data from the three units. The quality of the data from the HIRS/2 is consistent from unit to unit and is sufficient for supporting the operational system. Reliability of the systems have been excellent to date, indicating the ability to fully support the TIROS-N program.

1.0 SUMMARY

1.1 General

The High Resolution Infrared Radiation Sounder (HIRS/2) program activities included the development and test of three instruments for installation and long-term operation on the TIROS-N series satellite. The program began in July of 1976 to quickly provide a system for the TIROS-N satellite that would equal or improve upon the performance of a HIRS unit flown on the Nimbus 6 satellite in June of 1975. Many of the basic design features of the Nimbus HIRS were used in the new system. Other features had to be changed to meet the mechanical, electrical, and thermal interfaces of the new satellite. The protoflight instrument was completed and delivered on May 1, 1978, twenty-two months after contract award. The second unit, Flight Model One (FM1), was delivered on August 13, 1978, and the third unit, Flight Model Two (FM2), was delivered on February 14, 1979. The TIROS-N satellite was launched on October 13, 1978. After NASA control and checkout, the operation of the satellite was assumed by NOAA. HIRS/2 data were fed to the National Meteorological Center in mid-January and became part of the operational data on March 1, 1979.

This report includes a brief description of the instrument. Detailed material on the system and subsystem operation are given in the Technical Description for High Resolution Infrared Radiation Sounder Mod 2, October 1978. Other descriptive and test data are included in the "Instruction Manual and Calibration and Test Data Report" for each instrument. The final report will excerpt some of this data to compare the performance of the three units.

1.2 The HIRS/2 Instrument

The HIRS/2 program to provide an atmospheric sounding unit is derived from an instrument developed and flown on the Nimbus 6 satellite, Contract NAS5-21651. Results from orbital data and system study showed promise of obtaining data from which improved atmospheric soundings may be derived. The basic design of the Nimbus HIRS system was modified to accommodate the TIROS spacecraft and orbital requirements. Several changes in subsystem design were also made to improve the sensor performance and the reliability of the filter wheel drive assembly. A protoflight instrument was designed and assembled by using some parts from the HIRS/1 program. Later models used similar components with little change in design.

Multispectral data from one visible channel (.69 micron), seven shortwave channels (3.7 to 4.6 micron), and twelve longwave channels (6.7 to 15 micron) are obtained from a single telescope and a rotating filter wheel containing twenty individual filters. A mirror provides cross-track scanning of 56 increments of 1.8°. The mirror steps rapidly, then holds at each position while the filter segments are sampled. This action takes place each 0.1 seconds. The instantaneous field of view for each channel is approximately 1.2° which, from an altitude of 833 kilometers, is an area 17.45 kilometers in diameter at nadir on the earth.

Three detectors are used to sense scene radiation. A silicon cell detects the energy through the visible filter. An Indium Antimonide detector and a Mercury Cadmium Telluride detector mounted on a passive radiator and operating at 107K sense the shortwave and longwave energy. The silicon cell operating temperature is 288K. The shortwave and visible detectors share a common field stop, while the longwave uses a separate stop. Registration of the fields in all channels is determined by these field stops; secondary effects are caused by detector position.

Calibration of the HIRS/2 is provided by programmed views of three radiometric targets consisting of (1) an internal warm target mounted to the instrument base, (2) an internal cold target isolated from the instrument and operating at near 265K, and (3) a view of space. Data from these views provide sensitivity calibrations for each channel at 256 second intervals, if so desired. Internal electronic signals provide calibration of the amplifier chains at 6.4 second intervals.

Data from the instrument are multiplexed into a single data stream controlled by the TIROS Information Processor (TIP) system of the spacecraft. Information from the radiometric channels and voltage telemetry is converted to 13-bit binary data. Radiometric information is processed to produce the maximum dynamic range so that instrument and digitizing noises are a small portion of the signal output. Each channel is characterized by a noise equivalent radiance and a set of calibration data that may be used to infer atmospheric temperatures and probable errors.

The HIRS/2 instrument is a single package mounted on the Instrument Mounting Platform of the TIROS-N spacecraft. The unit is shown in Figures 1-1 and 1-2. A thermal blanket encloses most outer surfaces other than that of the radiating panel and door area. The radiating surface views space, emitting its heat to provide passive cooling of the detectors to the 107K temperature. A shield, which prevents thermal inputs from earth, is part of a door assembly that is closed during launch and is kept closed for an initial outgas period. At the end of that period the door is opened to allow the passive radiator to cool. If indications of contamination occur later in the operation of the system, the door remains open and heat is applied to bring both stages of the radiative cooler to near 300K.

Table 1-1 lists the general characteristics of the HIRS/2 Instrument. Table 1-2 lists the spectral channels and sensitivity characteristics for the HIRS/2. Figure 1-3 illustrates the pattern of scanning, showing the scan mirror and the positions of the calibration targets relative to earth scan.

A stepping mirror directs the radiant energy from the earth to a single, 6-inch diameter telescope assembly every tenth of a second. Collected energy is separated by a beamsplitter into longwave (above 6.5 μm) and shortwave (visible to 4.6 μm), then passed through field stops and through a rotating filter wheel to cooled detectors.

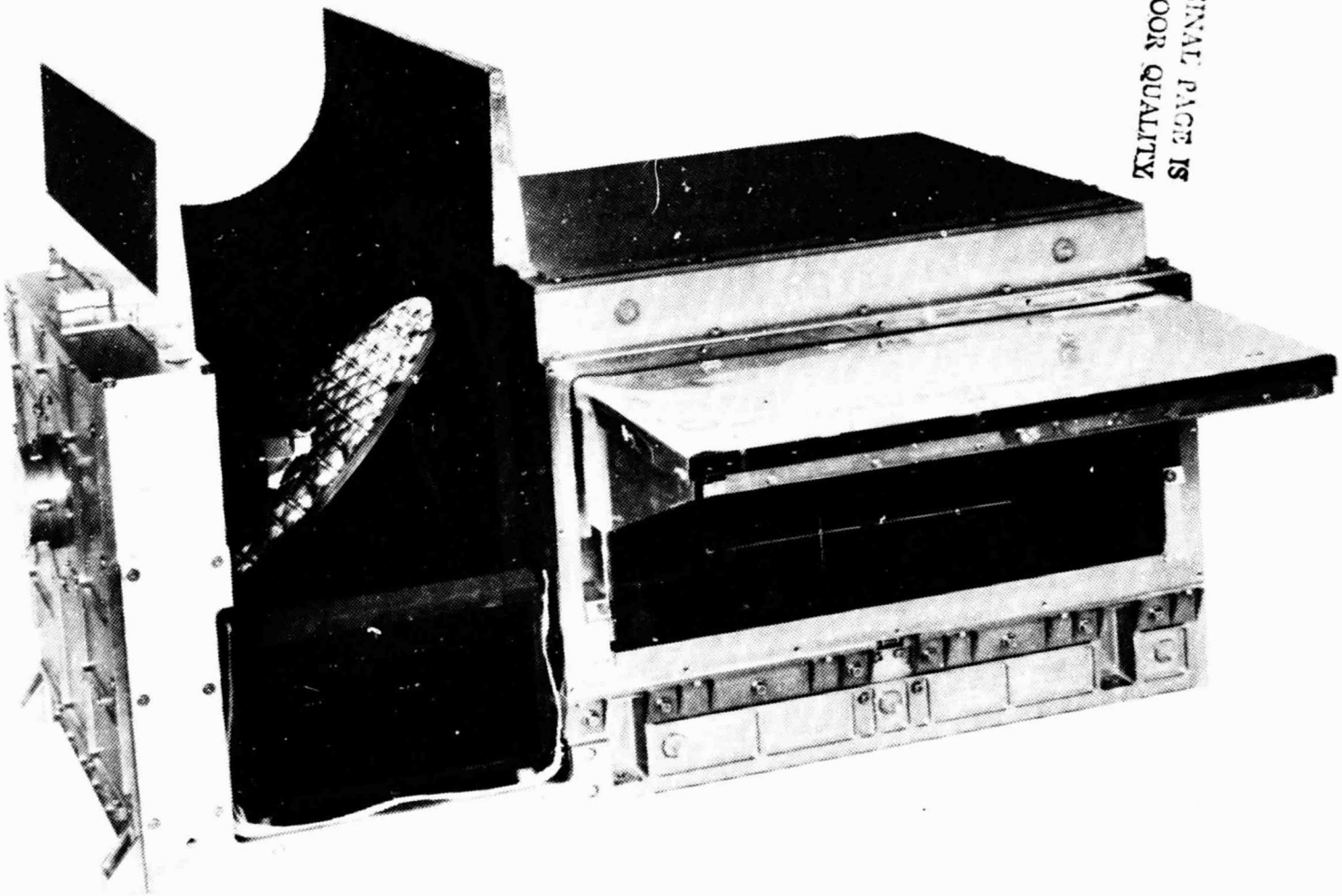

Figure 1-1. HIRS/2 Flight Model, Cooler View

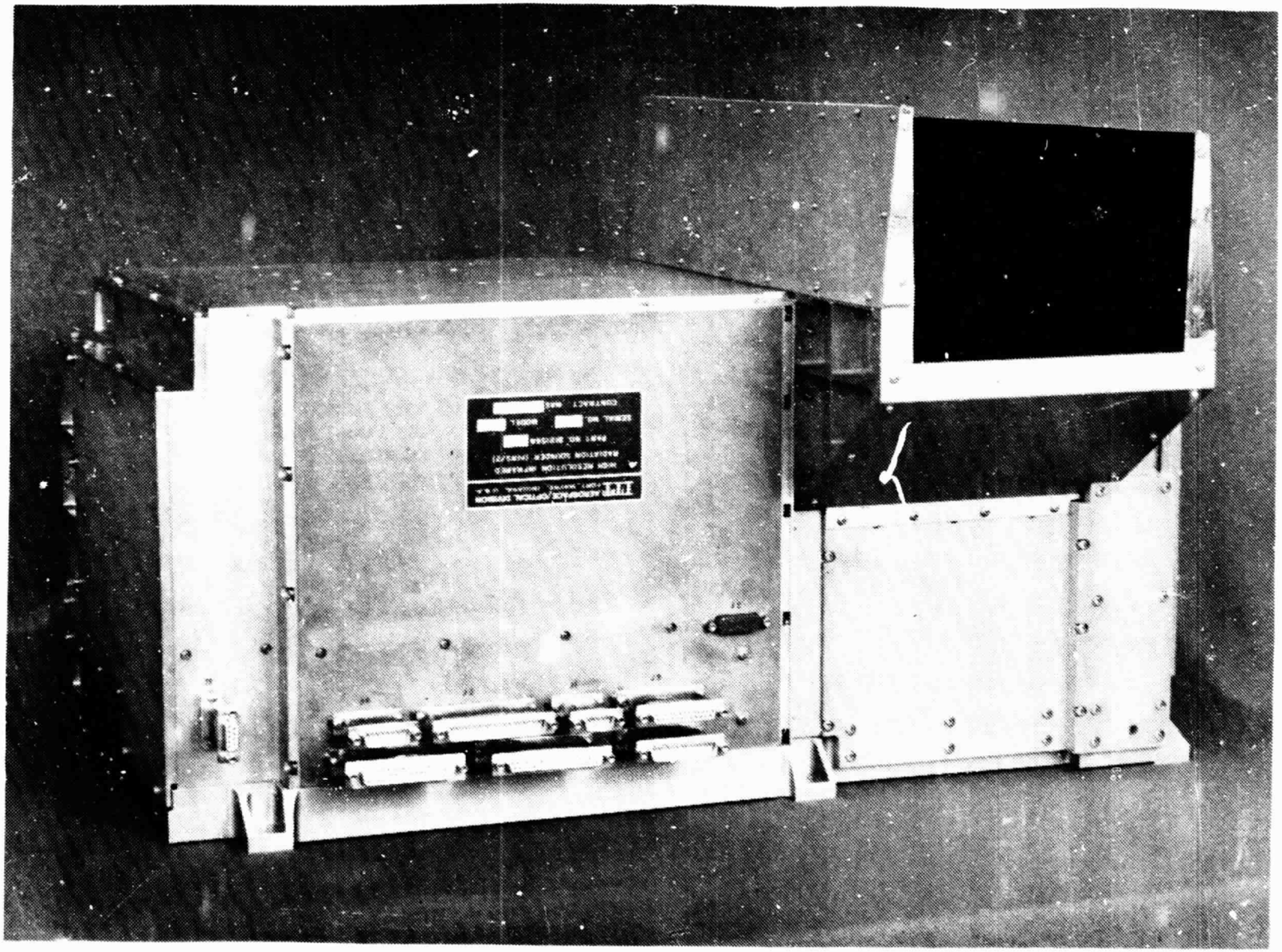

Figure 1-2. HIRS/2 Protoflight, Connector View

Table 1-1. HIRS/2 System Characteristics

Optic Field of View	1.22° typical
Included Energy	97% within 1.80°
Channel-to-Channel Registration	
Longwave	0.05 of FOV area, within band
Shortwave	0.02 of FOV area, within band
Earth Scan Angle	99.0°
Earth Scan Steps	56
Step and Dwell Time	100 ms total
Retrace Step Time Period	0.8s
Total Scan plus Retrace Time	6.4s
Earth Swath Coverage, 833 Km orbit	2254 km
Earth Field Coverage	17.5 km (1.22° FOV)
Radiometric Calibration	290K Black Body, 265K Black Body, and Space Look
Frequency of Rad. Cal.	256s, typical
Dwell Time at Cal. Positions	5.6s (4.8s at space)
Longwave Channels	12
Longwave Detector	Mercury Cadmium Telluride
Shortwave Channels	7
Shortwave Detector	Indium Antimonide
Visible Channel	1
Visible Detector	Silicon
Signal Quantizing Levels	8192 (13-bit coding)
Electronic Calibration	32 equal levels each polarity
Frequency of Elect. Cal.	One level each scan line (6.4s)
Telescope Aperture	15.0 cm (5.9 in)
IR Detector Temperature	107K
Filter Temperature	303K
Instrument Operating Temperature	15°C nominal

Table 1-2. HIRS/2 Spectral Characteristics

Channel	Channel Frequency (cm^{-1})	μm	Half Power Bandwidth (cm^{-1})	Maximum Scene Temperature (K)	System NEΔN PFM	FM1	FM2
1	669	14.95	3	280	2.56	2.47	3.18
2	680	14.71	10	265	.46	.63	.61
3	690	14.49	12	240	.53	.49	.43
4	703	14.22	16	250	.30	.34	.28
5	716	13.97	16	265	.19	.31	.19
6	733	13.64	16	280	.24	.35	.19
7	749	13.35	16	290	.14	.20	.14
8	900	11.11	35	330	.058	.068	.042
9	1,030	9.71	25	270	.030	.082	.055
10	1,225	8.16	60	290	.15	.16	.066
11	1,365	7.33	40	275	.14	.21	.14
12	1,488	6.72	80	260	.19	.17	.095
13	2,190	4.57	23	300	.0057	.0032	.0029
14	2,210	4.52	23	290	.0031	.0039	.0031
15	2,240	4.46	23	280	.0033	.0045	.0037
16	2,270	4.40	23	260	.0018	.0027	.0025
17	2,360	4.24	23	280	.0021	.0026	.0035
18	2,515	4.00	35	340	.0024	.0012	.0011
19	2,660	3.76	100	340	.0007	.00062	.00055
20	14,500	0.69	1000	100%A			

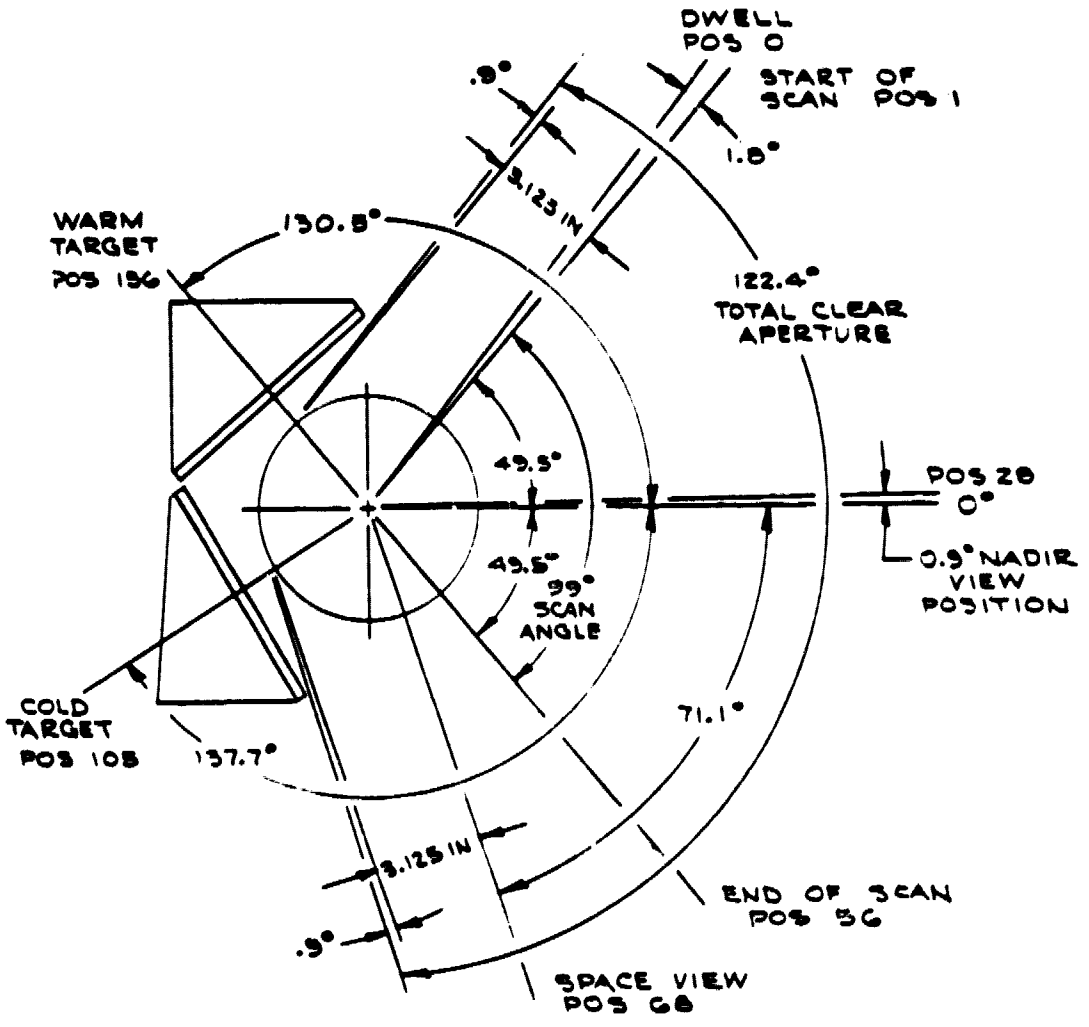

Figure 1-3. Scan Position

In the shortwave path, a second beamsplitter separates the visible channel to a silicon detector (See Figure 1-4).

The scan logic and control set the sequence of earth viewing steps to provide a rapid scan mirror step motion to 56 fixed positions for spectral sampling of each respective air column. The filter wheel rotation is synchronized to this step-and-hold sequence, with approximately one-third of the wheel blank so that the filters are positioned for sampling only after the mirror has reached the hold position. Registration of the optical fields for each channel to a given column of air is dependent to some degree on spacecraft motion and on the alignment of the longwave and shortwave field stops and on aberrations of the optic system.

Radiant energy is focused on cooled detectors operating at a near optimum temperature of 107K. A Mercury Cadmium Telluride detector and Indium Antimonide detector are mounted on a two-stage radiant cooler. This assembly is large enough to have reserve cooling capacity, permitting active thermal control to maintain the detectors at a fixed 107K. (1) The cooler and its housing are designed for contamination prevention. Windows on the housing and first stage prevent access of contaminants while controlling the heat input to the detectors. Baffles and traps aid capture of water vapor in other areas. A system of heating the second stage (patch) and first stage (radiator) is provided for initial outgassing and for decontamination later should it be desired. The cold first stage windows are heated several degrees above their surrounds to reduce collection of contaminants on those elements.

Electronic circuits provide the functions of power conversion, command, telemetry, and signal processing. Amplification of the inherently weak signals from the IR detectors is done in two low-noise amplifiers. The visible detector feeds a separate preamplifier but joins the shortwave chain just after the low-noise, shortwave preamplifier. Radiant signals are fed through a base reference and memory processor, multiplexed and A/D converted by a 13-bit range system. Once converted to digital format, the data are again multiplexed with HIRS/2 "housekeeping" data and provided as a serial data stream at the digital output. Data from HIRS/2 are held in memory until called by the TIROS Information Processor (TIP) request signals and clocked out of the instrument by the TIP clock. A simplified diagram of the HIRS/2 system is shown in Figure 1-5.

(1) Design changes made during testing of the protoflight unit included modification of the patch and first stage by mechanically stiffening them with thermally insulating rods. This reduced patch motion and the induced noise resulting from modulating the background radiation, but it also reduced cooling capacity of the system. This required a change in temperature control from 105K to 107K. At this temperature, the performance is slightly degraded and the cooling margin is less than initially planned.

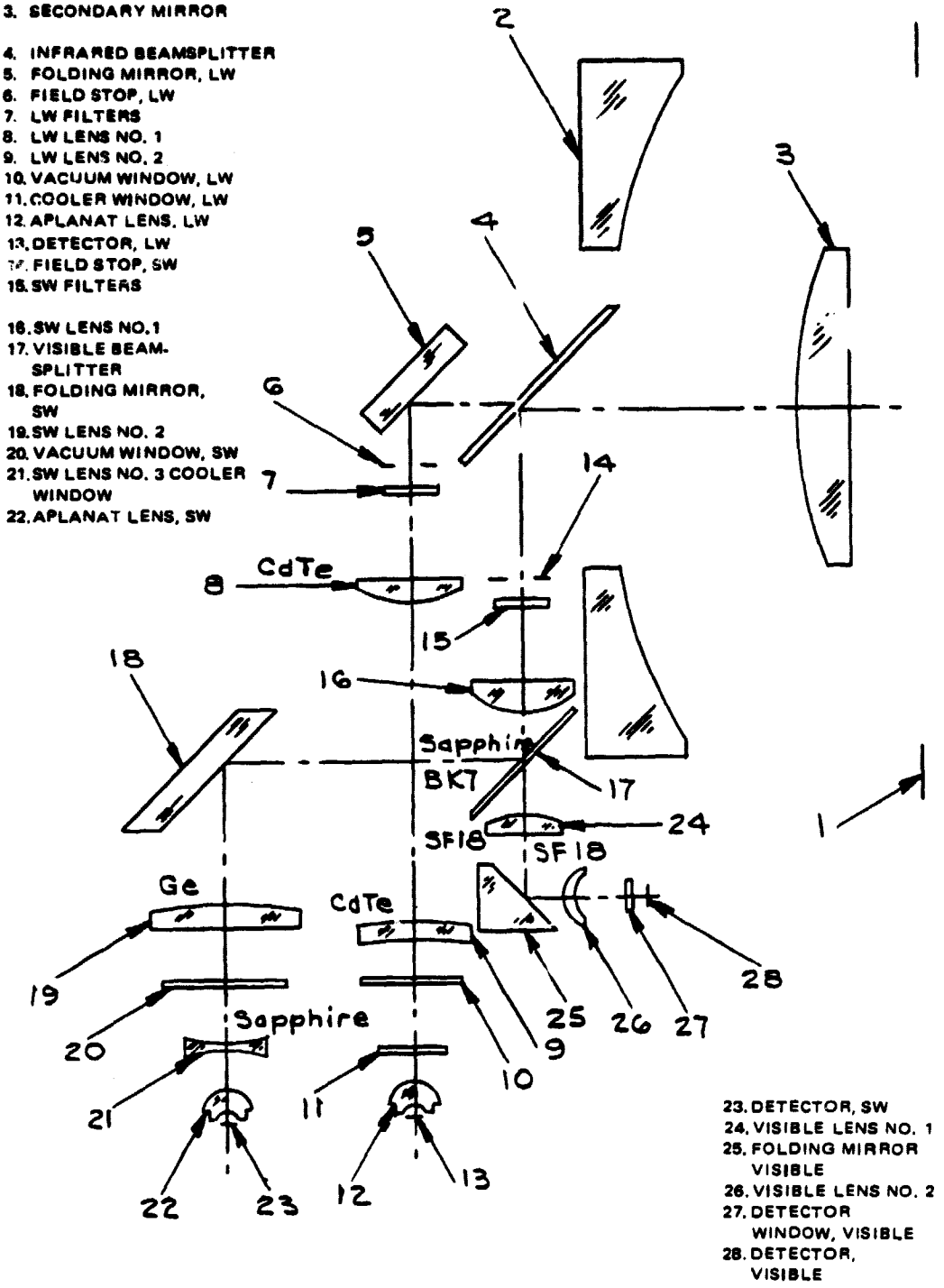

Figure 1-4. Optic Layout

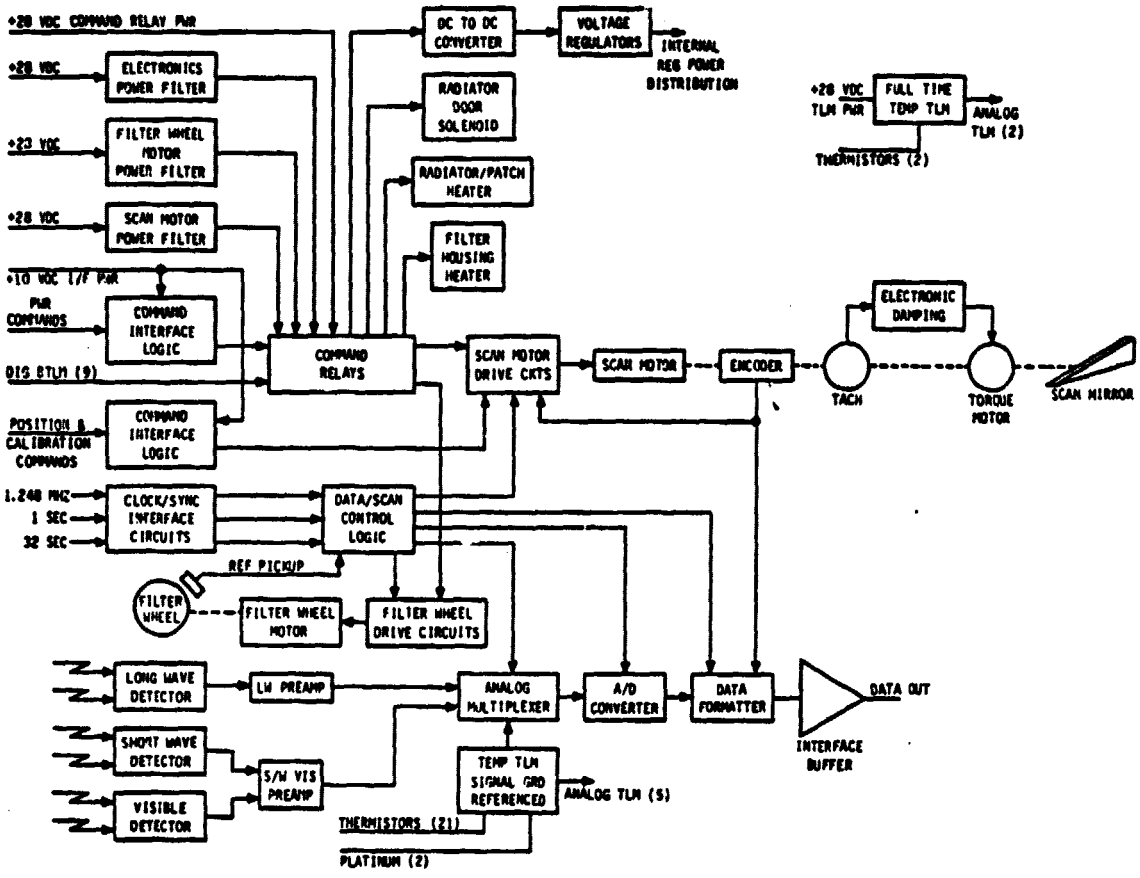

Figure 1-5. HIRS/2 System Block Diagram

Repetitive inclusion of electronic calibration signals and the periodic command to scan-to-space and two internal blackbodies provide the system with a complete set of data collection, calibration, and control that permits reliable operation in orbit.

General characteristics of the HIRS/2 instrument may be better understood through study of Figure 1-5 for electrical functions and Figure 1-6 which shows the major subassemblies of the instrument in an exploded view.

1.3 HIRS Program Schedule

The major events of the HIRS/2 development program are listed in Table 1-3. These are the more important milestones in the program and will be referenced in discussion of test data. The protoflight schedule was planned to deliver an operational instrument at the earliest possible time. Significant effort was expended accelerating the design and fabrication phase to meet a projected sixteen-month delivery schedule. Approximately two of the seven months of the schedule delay beyond the plan resulted from increased fabrication time and delays in component delivery from semiconductor manufacturers. The remaining delay occurred in the test period when signal noise levels were unexpectedly high. The investigation of the cause and modification of the assembly required two iterations of modification and test before achieving a reasonable system performance level. The protoflight unit, when delivered, had system noise levels above specification but within the baseline values of the Nimbus 6 HIRS system. Flight Model One assembly was slowed by the activity on the Protoflight Unit. During system tests, a special test was performed to verify the effect of radiance from outside the 1.8^{o} field of view. Total integrated flux had an effect of less than 1 percent of the scene flux. Modifications to FM1 are described in section 1.4.

The Flight Model Two schedule moved efficiently through the assembly and test periods; however, flight experience on TIROS-N increased concern for cooler margin of all units in orbit. The delivery of the FM2 was delayed several months while special instrumentation and tests were conducted to better define cooler thermal factors and validate the estimates of performance in orbit. From these tests, we made one modification to both FM1 and FM2 by adding a second shield on the cooler door. The final tests of FM2 were made with all modifications in place. These modifications are described in section 1.4.

Integration of the protoflight unit into the TIROS-N spacecraft took place after the normal spacecraft vacuum chamber test. In order to prove full instrument performance on the spacecraft with the detectors cold, a special test assembly was fabricated. This test assembly functioned satisfactorily but was difficult to set up and required careful handling to prevent damage to the instrument. The test was under spacecraft control and did confirm normal operation with the other TIROS-N systems.

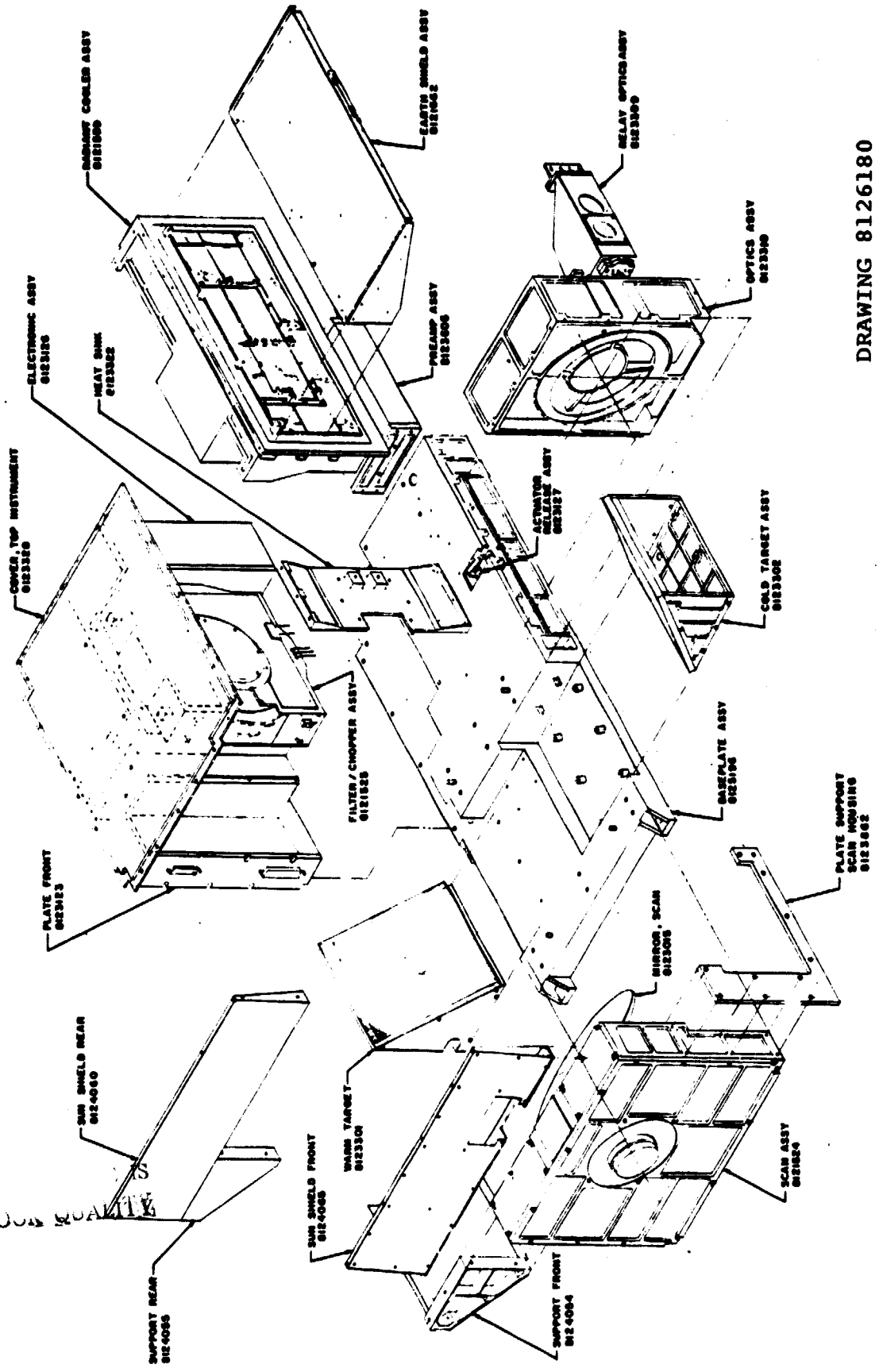

DRAWING 8126180

Figure 1-6. HIRS/2 Subassemblies

Table 1-3. HIRS/2 Program Chronology

June 29, 1976	Contract Start Date
October 5, 6, 7	Preliminary Design Review
February 24, 25, 1977	Critical Design Review
September 17	Protoflight System Assembled
October 5, 6	Final Design Review
November 19-21	First Chamber Test
December	Investigation of noise sources
January 12-16, 1978	Chamber Tests
January 18, 19	First Vibration Test
March 3	Patch modified to reduce vibration
March 15	Chamber and Vibration Test
April 5	Motor bearing changes and vibration retest
April 10-24	Chamber Calibration Tests
May 1	Protoflight delivery to RCA
May 7	FM1 system assembly complete
May 22	PFM cooled detector tests on S/C complete
May 25, 26	Post Environmental Review
July 13-22	FM1 Chamber Test
July 29	Vibration Test
August 3-17	Chamber Calibration Tests
August 24	FM1 delivery to RCA
October 13	Launch of TIROS-N
October 28 - December 17	FM2 Pre-vibration chamber tests
October 30	PFM full operation on TIROS-N
January 8, 1979	FM2 Vibration Tests
January 14-28	Chamber Calibration Tests
January 30 - February 11	Special chamber tests
February 19	Deliver FM2 to RCA
June 27	Launch of NOAA-6

Flight Models One and Two were both delivered to the integrator's facilitiy in time to be mounted to the spacecraft before chamber test; this eliminated the need for the special cooler test.

1.4 Physical Differences Between Units

The three instruments delivered on the HIRS/2 development contract are basically the same. Some differences occurred in the use of HIRS/1 components for the protoflight unit and the modification of Flight One and Flight Two to improve system performance.

1.4.1 Optics

In order to reduce procurement time and cost, some residual items from the HIRS/1 program were used in the protoflight model. Major items were the scan mirror, telescope, visible detector, some spectral filters and some optic elements. Tables 1-4, 1-5 and 1-6 list the optic elements in each unit for the longwave, shortwave, and visible paths, respectively. When parts for Flight One were procured, the telescope was purchased from Perkin-Elmer Corporation rather than from Ferson Optics. The prescription remained the same, but the black surfaces of the dichroic assembly were black painted rather than black iridited to reduce reflection. A special baffle to reduce potential light entry to the field stop was added to the protoflight unit and included in the flight unit design.

1.4.2 Cooler Door

Two changes have been made to the cooler door (earth shield) to improve its effectiveness and reliability.

As the result of design changes to the protoflight patch to add stiffener rods, the door is prevented from closing to its typical position parallel to the cooler surface. At an angle of ten degrees, the door required a lengthened strap between the door and latch. The change in strap length was made on the protoflight, but problems encountered in vibration led to further redesign. After premature opening at TIROS-N launch, the design was changed to increase the strength of the strap and preclude bending during closure or operation. The PFM and FM configurations are shown in Figure 1-7. This change was retrofitted on FM1 at the integrator's facility and included on FM2 before delivery. No problems were encountered during the launch of FM1 on NOAA-6.

A second shield was added to the door to reduce the earth and solar input to the cooler door that is coupled to the cooler radiator. The original shield remained in place, but spacers and a second shield were added as shown in Figure 1-8. This reduced the radiant input sufficiently to provide a predicted gain of nearly four milliwatts of patch cooling capacity. The shield was added to FM1 at the integrator's facility. On FM2, the shield was added before the final chamber thermal tests at ITT; this permitted checking performance before delivery.

Table 1-4. HIRS/2 Longwave Optics

ELEMENT DESCRIPTION	MATERIAL	PROTOFLIGHT			FLIGHT ONE		FLIGHT TWO	
		HIRS/2 DRAWING NUMBER	SOURCE	SERIAL NUMBER	SOURCE	SERIAL NUMBER	SOURCE	SERIAL NUMBER
SCAN MIRROR	BERYLLIUM	8123015	APPLIED OPTICS	8117351*	APPLIED OPTICS	3	APPLIED OPTICS	102
PRIMARY MIRROR	CERVIT	8123272	FERSON	9254101*	PERKIN-ELMER	001	PERKIN-ELMER	002
SEC. MIRROR	CERVIT	8123265	FERSON	9254102*				
BEAM SPLITTER	GERMANIUM	8123262	OCLI	9254119*	OCLI	---	OCLI	---
FOLDING MIRROR	PYREX	8123263	FERSON	9254104*	PERKIN-ELMER	001	PERKIN-ELMER	002
L.W. LENS #1	CDTE	8123047	II-VI	S/N 684-T1	II-VI	761-3	II-VI	751-B
L.W. LENS #2	CDTE	8123048	II-VI	S/N 631-C	II-VI	752-B	II-VI	752-C
L.W. VACUUM WINDOW	CDTE	8123108	II-VI	S/N 600-6B	II-VI	731A-2	II-VI	728-10
L.W. RADIATOR WINDOW	ZNSE	8123049	II-VI	S/N 2068-32	II-VI	2655-17	II-VI	2537-10
L.W. APLANAT	GERMANIUM	8121550	FERSON	9254108*	HIBSHMAN		HIBSHMAN	
L.W. DETECTOR	HgCdTe	8122972	HONEYWELL	SN/1	HONEYWELL	2	HONEYWELL	5

*FERSON DRAWING NUMBER FOR PARTS FROM HIRS/1 FLIGHT MODEL

Table 1-5. HIRS/2 Shortwave Optics

		PROTOFLIGHT			FLIGHT ONE		FLIGHT TWO	
ELEMENT DESCRIPTION	MATERIAL	HIRS/2 DRAWING NUMBER	SOURCE	SERIAL NUMBER	SOURCE	SERIAL NUMBER	SOURCE	SERIAL NUMBER
SCAN MIRROR	BERYLLIUM	8123015	APPLIED OPTICS	8117351*	APPLIED OPTICS	3	APPLIED OPTICS	102
PRIMARY MIRROR	CERVIT	8123272	FERSON	9254101*	PERKIN-ELMER	001	PERKIN-ELMER	002
SEC. MIRROR	CERVIT	8123265	FERSON	9254102*				
BEAM SPLITTER	GERMANIUM	8123262	OCLI	9254119*	OCLI	---	OCLI	---
S.W. LENS #1	SAPPHIRE	8123017	FERSON	9254109*	EXOTIC	199-1	EXOTIC	199-2
SW/VIS BEAM SPLITTER	BK-7	8123269	OCLI	9254112*	VALPEY	211-1	VALPEY	211-2
S.W. FOLDING MIRROR		8123266	FERSON	9254113*	VALPEY	7	VALPEY	211-2
S.W. LENS #2	GERMANIUM	8123016	EXOTIC	S/N 1	EXOTIC	2	EXOTIC	3
S.W. VACUUM WINDOW	ZnSe	8123018	II-VI	S/N 2131-62	EXOTIC	199-1	EXOTIC	199-4
S.W. LENS #3	SAPPHIRE	8123019	OCLI	9254121*	VALPEY	199-2	VALPEY	199-1
S.W. APLANAT	GERMANIUM	8121549	FERSON	9254116*		#7		
S.W. DETECTOR	InSb	8122970	CINCINNATI ELEC.	S/N 1	CINCINNATI	#10	CINCINNATI	23

*FERSON DRAWING NUMBER FOR PARTS FROM HIRS/1 FLIGHT MODEL

Table 1-6. HIRS/2 Visible Optics

		PROTOFLIGHT			FLIGHT ONE		FLIGHT TWO	
ELEMENT DESCRIPTION	MATERIAL	HIRS/2 DRAWING NUMBER	SOURCE	SERIAL NUMBER	SOURCE	SERIAL NUMBER	SOURCE	SERIAL NUMBER
SCAN MIRROR	BERYLLIUM	8123015	APPLIED OPTICS	8117351*	APPLIED OPTICS	3	APPLIED OPTICS	102
PRIMARY MIRROR	CERVIT	8123272	FERSON	9254101*	PERKIN-ELMER	001	PERKIN-ELMER	002
SEC. MIRROR	CERVIT	8123265	FERSON	9254102*				
BEAM SPLITTER	GERMANIUM	8123262	OCLI	9254119*	OCLI	---	OCLI	---
S.W. LENS #1	SAPPHIRE	8123017	FERSON	9254109*	EXOTIC	199-1	EXOTIC	199-2
SW/VIS BEAM SPLITTER	BK-7	8123269	OCLI	9254112*	VALPEY	211-1	VALPEY	211-2
VIS. LENS #1	SF 18	8123267	FERSON	9254110*	VALPEY	211-1	VALPEY	211-2
S.W. FOLDING MIRROR	PYREX	8123264	FERSON	9254118*	VALPEY	211-1	VALPEY	211-2
VIS. LENS #2	SF 18	8123268	FERSON	9254111*	VALPEY	211-1	VALPEY	211-2
DET. WINDOW	QUARTZ	8123352	ELECTRO-NUCLEAR	8117812*	ELECTRO-NUCLEAR	42	ELECTRO-NUCLEAR	41
VISIBLE DETECTOR	SILICON							

*FERSON DRAWING NUMBER FOR PARTS FROM HIRS/1 FLIGHT MODEL

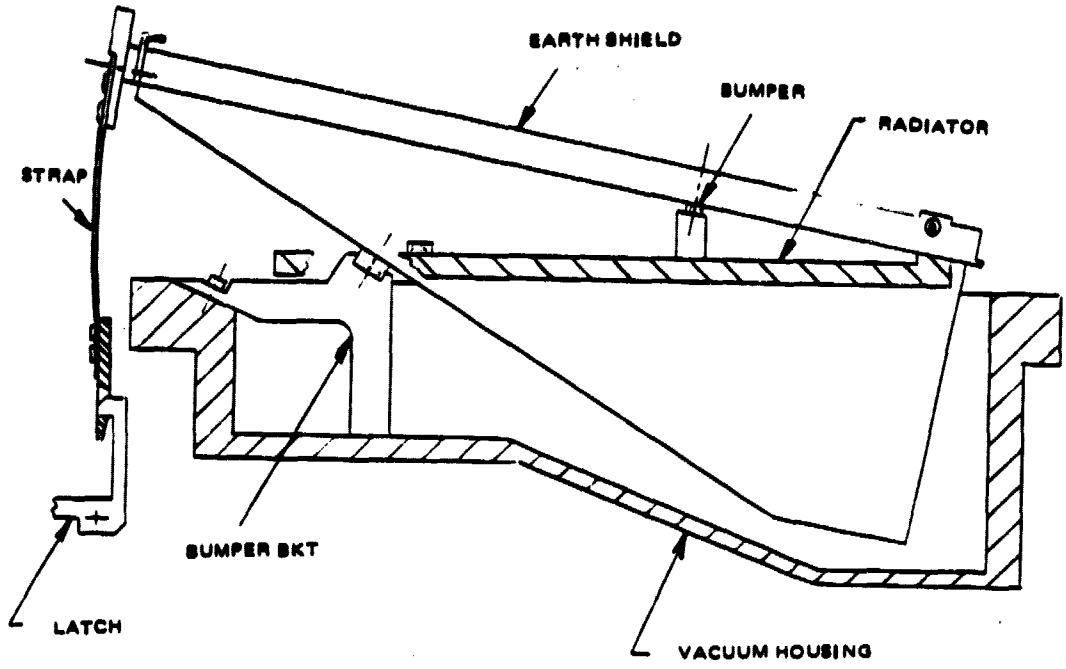

Figure 1-7A. PFM Cooler Configuration

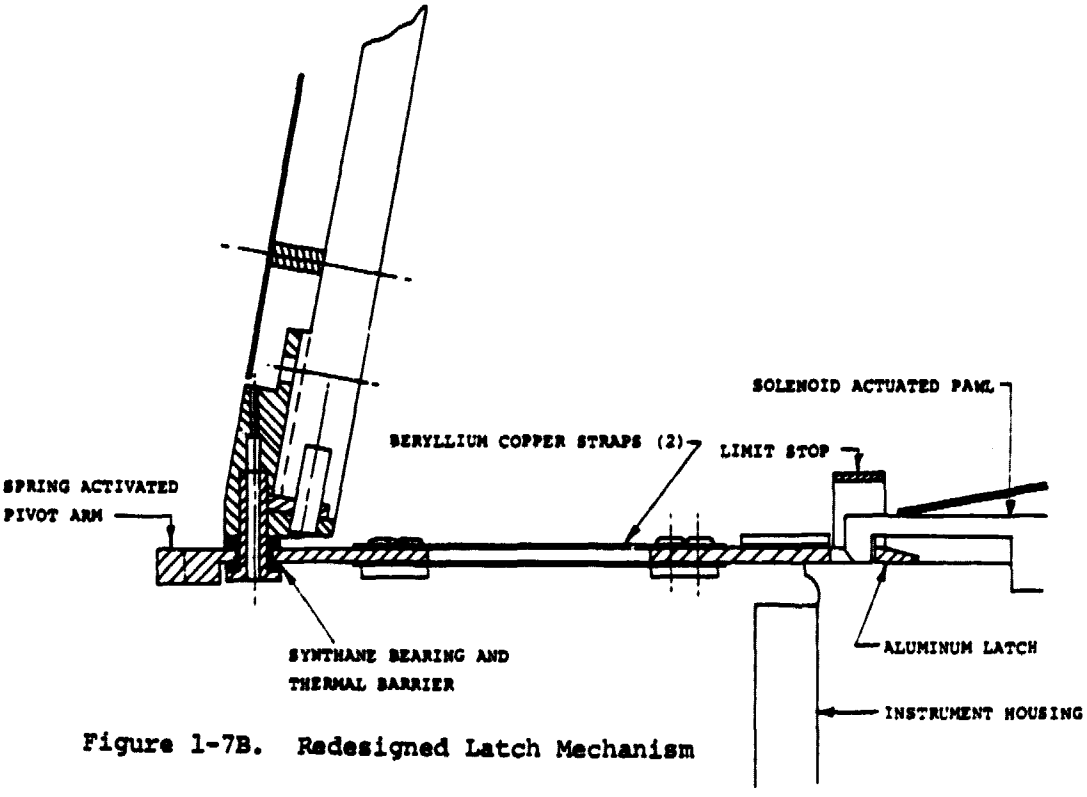

Figure 1-7B. Redesigned Latch Mechanism

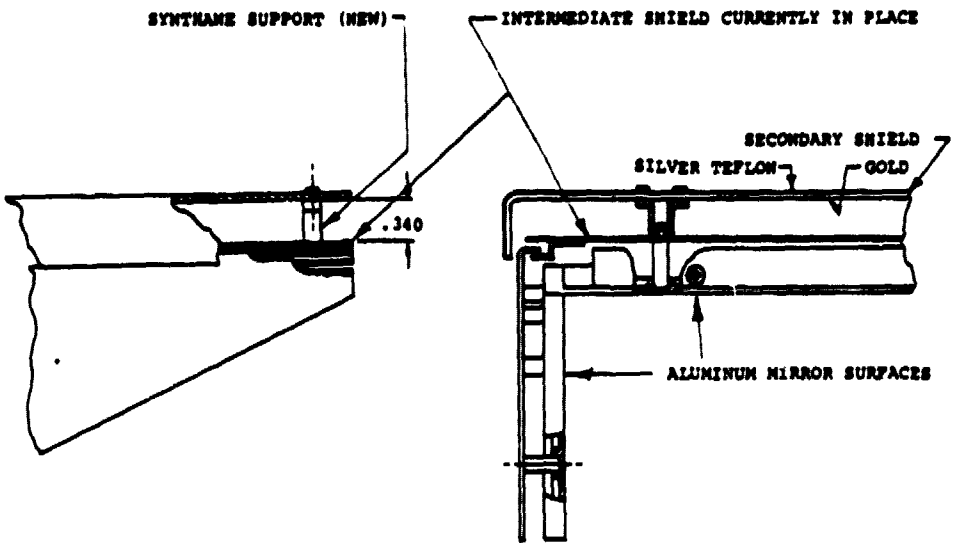

Figure 1-8. Second Shield Added To Earth Door

1.4.3 Scan Cavity Sun Shield

An additional shield was added to the scan cavity (as shown in Figure 1-1) forming the circular opening above the warm calibration target. It restricts solar input more completely than before the change. This shield was added to FM1 at the integrator's and to FM2 before delivery.

1.4.4 Cooler Housing Temperature Monitor

An available temperature telemetry position in the data stream was implemented to monitor the cooler housing temperature. A thermistor mounted on the vacuum housing is used to check the housing temperature to verify the heat flow into the cooler assembly. The information is not used in system calibration, but aids thermal modeling and test evaluation. This change is in both flight models but not in the protoflight unit.

1.4.5 Relay Block Inserts

Tests for noise sources indicated that energy emitted from the interior surfaces of the relay housing block were being reflected from the filter wheel back to the detector. Aluminized mylar sleeves with the aluminum surface toward the optic column were inserted in the cylindrical cavities of the relay block and held in place by adhesives. The effect of the change was noticeable as a reduction of background noise in the shortwave system. Both the FM1 and FM2 have this change.

1.4.6 Longwave Detector and Aplanat

Optical analyses verified that the detector and aplanat both have large numbers of rays striking their surfaces at high incidence angles. The surface antireflective coating of the detector was changed accordingly to aid collection of high incidence angle rays. This change was incorporated in the detectors for both flight models. At the same time, a program was started to define and change the coating on the aplanatic lens that mounts to the detector. This change could not take place in time for FM1 or FM2. The next unit, FM3 will have both the improved detector surface and improved aplanat surface.

1.4.7 Outgas Heater Control

The ability to correctly simulate thermal inputs to the cooler radiator and patch was hampered by the limitations on test equipment and methods. In FM2, the wiring to the radiator and patch outgas heaters was modified to have the wires exit the instrument through an available unused connector. External resistance and current monitors could then be included in the line for adjustment of heat input to these components. This permits selection of thermal loads simulating various orbit angle solar inputs. The result was test data more accurate and effective in prediction of cooler performance in orbit. After test, the connector has a mating plug with loop-through wiring that returns the wiring to its original internal circuit. This change is incorporated in Flight Model Two only.

2.0 SYSTEM PERFORMANCE

The performance of the three HIRS/2 units will be given here as an indicator of the final operating conditions before delivery. Only the major items of final test data will be presented. Detailed information has already been published in the Instruction Manuals, Test Reports, and Calibration and Test Reports of the respective units.

2.1 Functional Performance

System level tests of each unit include checks of all calibration and functional data and measurement of parameters during each operating mode and at each test temperature.

Scan system performance was excellent throughout all instrument operation and test. The step performance of all units was within specification on final tests. Long period data monitoring at the integrator detected two infrequent scan retrace anomalies. In one case, the scan logic reacted to chatter in encoder reference signals, preventing proper retrace to the zero position. In the second case, a gating signal had too narrow of a tolerance, causing an extra step to be included at the end of a calibration sequence. Tests at ITT determined the causes of the problems. A component value change and a circuit modification were made to the Protoflight model (PFM) and subsequent units. After this change, there were no identifiable scan anomalies in instrument test or orbit operation.

Filter wheel motor performance was equally successful, with no reported failures or loss of synchronization that could be attributed to the filter wheel drive control. (A number of apparent failures were found to be related to computer data processing errors.) Tests of the filter wheel drive under cold conditions resulted in motor start at 5°C, the lowest required temperature for system performance.

Filter housing temperature is automatically controlled at 30°C. This temperature control system works extremely well by maintaining the housing to within 0.01°C. Under warm instrument conditions, system tests were conducted at a baseplate temperature of 25°C. It was found that the filter motor added sufficient heat to raise the housing above its normal control temperature of 30°C. At a baseplate temperature of 22°C, the housing came into control. A special test with heat control turned off showed that the well-insulated housing remains stable over long periods with no added heat input. A test of FM1 in the ITT chamber with filter housing heat off indicated a stable 294K temperature and a reduced noise level. In orbit, this performance was duplicated, resulting in a decision to consider this the nominal operating condition for mission mode.

Electronic calibration is included in the system data after each scan line. Tests of linearity and stability under temperature and time conditions show this input to be sufficiently accurate so that no linearity correction need be included in the data processing. Long-term stability of this system has been excellent.

Each voltage source in the instrument is monitored once per line (6.4 seconds). These data are reviewed for deviations in voltage at each test condition. There have been no malfunctions or deviations of the voltage supplies or monitoring system during any of the system tests or in orbital operations to date.

Electrical tests for power supply transients showed the protoflight slightly out of specification because of current transients occurring during scan system braking. In Flight Models One and Two, the scan control system was optimized slightly and resulted in bringing these transients within specifications.

2.2 Scan Plane Alignment

Tests of the deviation of the scan angle from its desired position show the effect of the mounting of the scan housing, baseplate, and mirror with respect to the optic axis. The results of the tests on the three units is shown in Figure 2-1. It may be noted that the error shown in the protoflight unit is all in one direction. On the later units, the alignment procedures were improved to permit a reduction of the error and a better centering around the zero error condition.

2.3 Instrument Weight

The protoflight and flight models were weighed before shipment to the integrator. FM2 had the extra door shield before shipment. Weights of the three units are given below.

Protoflight	71.50 pounds
Flight One	71.25 pounds
Flight Two	71.62 pounds

2.4 Cooler Performance

Performance of each radiant cooler was measured in a chamber test. The coolers were operated under conditions that simulate space as nearly as possible. In each test, the patch and radiator view a liquid helium temperature target. Solar and earth inputs were simulated on the protoflight through controlled thermal input by means of radiation from a special source close to the cooler door. For FM2, the solar and earth inputs were applied by electrically heating the patch and radiator. This gave more precise control of these inputs. The tests of FM2 then permitted a more accurate thermal model to be formulated for the instrument as shown in Table 2-1. The characteristics of the system derived from this model are given in Table 2-2. Note that FM1 was modified at the integrator's facility so that its thermal properties are the same as FM2. The differences in performance are related to (1) normal construction tolerances, (2) the differences in detector bias power, and (3) the control temperature set by circuit parameters.

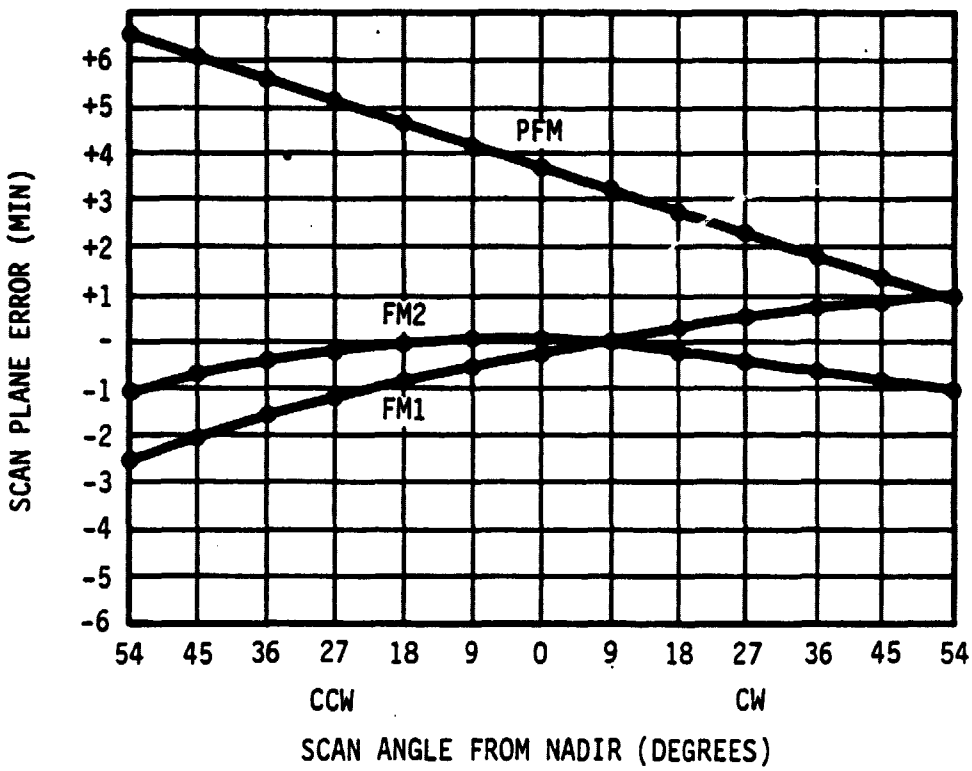

Figure 2-1. Scan Plane Alignment

Table 2-1. HIRS/2 Cooler Thermal Model

	45° Orbit 15° Base	68° Orbit 15° Base
PATCH TEMPERATURE	106.7 K	106.7 K
Power Radiated	103.0 mW	-103.0 mW
Support Rods	12.0	13.8
Gold Back	13.0	16.7
Detector Bias	18.0	18.0
Optical Input	17.0	18.1
Shield Radiative	11.3	16.0
Extra Rods	17.3	19.6
Control Power	14.3 (3.5°)	0.7
RADIATOR TEMPERATURE	170.5 K	179.9 K
Power Radiated	-1.19 W	-1.47 W
Strap Input	.127	.430
Multilayer	.345	.334
Support Rods	.217	.248
Optical Input	.311	.311
Shield Radiative	.013	.019
Earth Input	.152	.170
Patch Loss	-.028	-.035
DOOR TEMPERATURE	173.1 K	188.5 K
Solar Input	.053 W	.445 W
Strap Loss	-.127	-.430
Cover Input	.172	.125
Radiator Radiated	.012	.015
Power Radiated	-.111	-.156

Table 2-2. HIRS/2 Cooler Performance

	Predicted From Thermal Model		Test From Chamber (Corrected for 45 Orbit)			Actual From Orbit 11/28/78	7/13/79	
	PFM	ALL FM	PFM	FM1	FM2	PFM	FM1	
Patch Sensitivity(1)	.27	.25	.25	.25	.25			K/mW
Radiator Sens. (1)	21.5	21.5	22.5	21.5	21.5			K/W
Patch/Radiator Coupling (1)	.26	.26	.18	.26	.26			K/K
Radiator Temperature	173.7	170.5	173.8	171.0	171.8	178.6	176.4	K
Patch Control Temp	106.5	106.7	106.6	106.6	106.3	107.5	106.6	K
Patch Control Power Measured			7.9	10.2	12.9			
Patch Control Power (45° Orbit)	10.0	14.3	9.1	12.8	15.5	0.0	8.7	mW
Sun Angle	45	45	45	45	45	45	35	Deg
Decontamination Temp Patch (Door Open)	300.2	298.0	288.4			280.0	291.9	K
Radiator (Door Open)	304.3	299.8	298.1			300.9	301.6	K

(1) Accurate values not obtainable from orbital data.

Since door shields were changed on FM1 and FM2, but not on the Protoflight Model, a correction factor is applied to the Protoflight Model for this effect.

Cooler test data for Protoflight Model, FM1, and FM2 may be compared for cooling capacity if corrections are made for known changes in (1) longwave detector bias power, (2) the door changes mentioned above, and (3) the slight differences in patch control temperature. Using the Protoflight Model as reference, we can tabulate the variations and have a relative evaluation of the coolers. The test data shown in Table 2-3 are for chamber tests approximating a 45° solar input condition and with no corrections made for orbit versus chamber conditions. The standardized results show only 4.0 mW variation between units and indicate that FM1 and FM2 are equivalent thermally. It does not indicate that their performance will be the same in orbit.

Table 2-3. Cooler Capacity

	TEST			CORRECTION			
	RAD TEMP	PATCH TEMP	PATCH PWR	BIAS PWR	PATCH TEMP	DOOR	RESULT
PFM	173.8K	106.6K	7.9 mW	0	0	+4.8	12.7 mW
FM1	173.7	106.6	10.2	-1.3	0	0	8.9
FM2	170.5	106.3	12.9	-5.4	+1.2	0	8.7

The Protoflight Model unit on TIROS-N experienced a failure of the door latch mechanism at shroud ejection, resulting in premature cooling of the system. Shortly after this occurrence, cooler heat was applied but the spacecraft lost attitude control and began rotating, exposing the cooler to solar input. To conserve power, the instrument and its outgas heater were then turned off, again resulting in rapid cooling. When spacecraft stability was recovered, the cooler heat was restored and the two-week outgas period continued. The loss of cooling capacity shown in Table 2-2 as well as the difference noted in Table 2-3, may be attributed to contamination captured during the early cold intervals; this loss may, in part, be caused by a portion of the latch mechanism remaining in the field of view of the patch.

FM1 achieved proper outgassing temperatures of 310K on the patch and 294K on the radiator with the door closed. Concern for potential degradation of the longwave detector at temperatures above 293K led to opening of the door after four days. The cooler heat was turned off after 14 days. After cooling for two days, the radiator stabilized near 176.4K, about 5.4K above prediction.

A comparison of predicted-to-actual cooling capacity needs a correction for sun angle. At 45°, the solar input to the radiator was predicted at 53 mW. At 35°, the input is near 20 mW. The 33 mW difference can be translated to patch cooling capacity using the coupling and sensitivity factors given in Table 2-2.

$$33 \text{ mW} \times \frac{21.5\text{K}}{\text{W}} \times \frac{.26\text{K}}{\text{K}} \times \frac{1 \text{ mW}}{.25\text{K}} = 0.74 \text{ mW}$$

Subtracting this from the 8.7 mW actually achieved brings the patch control power to 8.0 mW. The 5.4K higher temperature of the radiator increases patch losses another 5.6 mW so that, if the radiator had performed as expected, the equivalent patch control power would be 13.6 mW as compared with 12.8 mW predicted. This indicates patch cooling capacity very close to the projected value and radiator cooling capacity below projected.

2.5 Optics

The optic systems all have the same basic design, but show differing test performance because of variabilities of the optic parts, field stops, and detectors. The optical parts are listed in Tables 1-4, 1-5, and 1-6, and in more detail in the Technical Description. In PFM and FM1, the field stop diameter was reduced to 0.222 inches to improve registration by reducing the effect of optic and detector vignetting, while in Flight Two the original 0.262 inch aperture is used at the expense of some vignetting and longwave-to-shortwave misregistration. It made the alignment of these detectors more difficult, but resulted in a noticeable increase in field of view sizes. A change in sounding algorithms by NOAA, reducing the dependence on longwave-to-shortwave registration, permitted the two bands to be optimized independently.

Measurement of optical field of view is made with the instrument in a fully assembled condition. A computer-controlled two-axis motion system moves a radiant source to 400 positions in a 1.8° field. Data is taken from all channels and fed to the computer where the best fit circle is generated for the 50 percent amplitude condition and for the Effective Field of View (EFOV). The EFOV is the diameter of a cylinder within which all energy would be contained at peak amplitude. The centroid of the energy is also calculated and plotted to indicate relative positions of the optical fields for each channel. The results of these tests are shown in Figure 2-2. Alignment of the FM2 optics and detector were accomplished to obtain the largest fields of view with reduced concern for registration of longwave-to-shortwave channels because the sounding algorithms no longer assumed perfect registration. For FM2, we concentrated on obtaining maximum throughput with only nominal effort to register the channels. As noted in Table 2-4, the field sizes did increase and registration is worse than that on prior systems.

The uniformity of energy within the optic field has been consistently poor in the longwave channels and excellent in shortwave

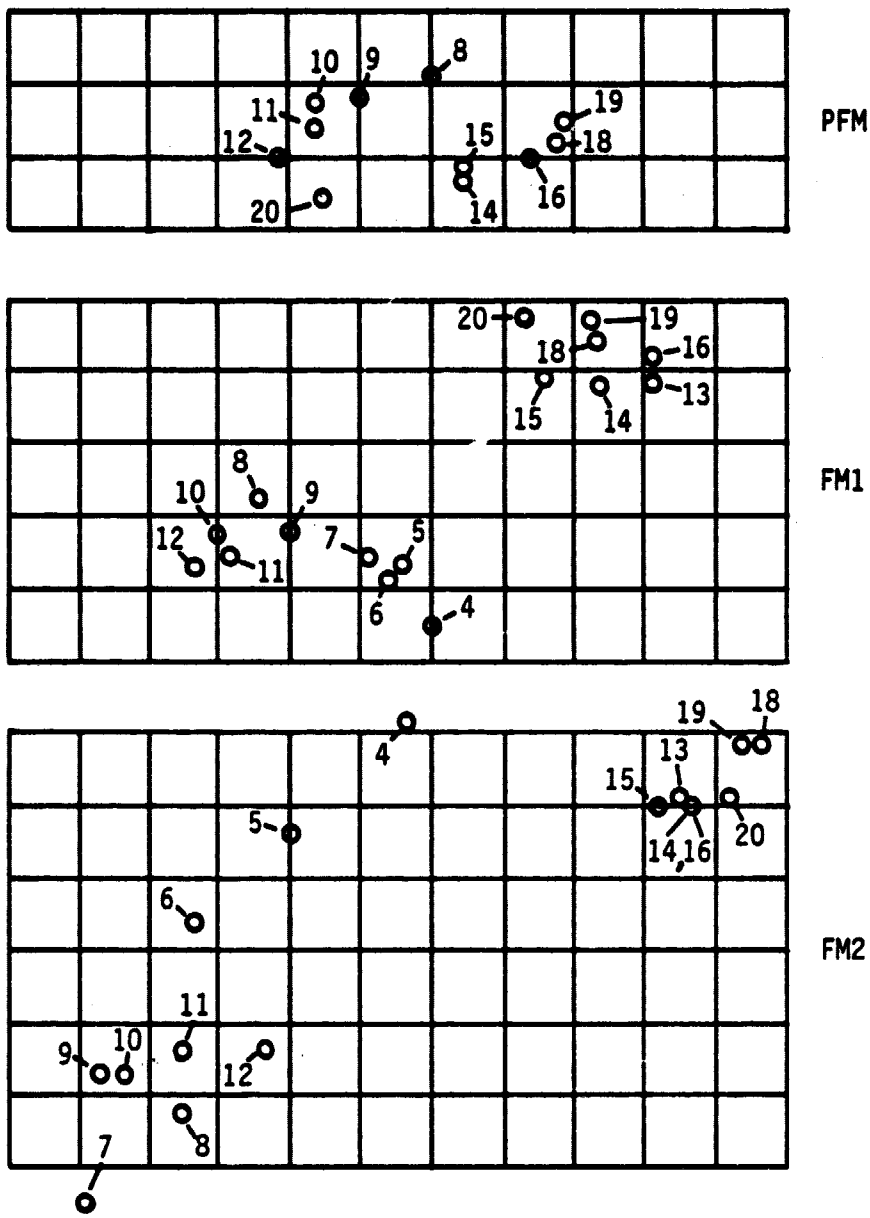

Figure 2-2. Optical Registration, Relative Centroid Positions; .01° Grid

Table 2-4. Optical Field of View Data

Field of View Diameter (Degrees)

Channel Numbers		50% FOV			EFOV		
		PFM	FM1	FM2	PFM	FM1	FM2
LW	1	-	-	-	-	-	-
	2	-	-		-	1.14	-
	3	1.18	1.16	1.33	1.15	1.14	1.28
	4	1.17	1.17	1.33	1.14	1.14	1.29
	5	1.18	1.17	1.33	1.15	1.14	1.29
	6	1.18	1.17	1.30	1.15	1.14	1.28
	7	1.19	1.18	1.29	1.15	1.14	1.27
	8	1.20	1.20	1.29	1.17	1.15	1.29
	9	1.21	1.21	1.26	1.18	1.16	1.22
	10	1.21	1.20	1.26	1.16	1.15	1.26
	11	1.20	1.20	-	1.16	1.15	-
	12	1.20	1.19	-	1.15	1.13	-
SW	13	-	1.23	-	-	1.19	-
	14	-	1.23	-	-	1.20	-
	15	-	1.23	-	-	1.21	-
	16	-	1.23	-	-	1.21	-
	17	-	1.22	-	-	1.19	-
	18	1.23	1.24	1.44	1.22	1.21	1.39
	19	1.24	1.23	1.45	1.22	1.21	1.40
VIS	20	1.22	1.22	1.51	1.17	1.22	1.43

NOTE: Data from some channels unobtainable in final HIRS/2 configuration.

and visible. This characteristic has been a strong influence in the inability to register the two infrared bands. Figure 2-3 shows these characteristics for typical longwave and shortwave channels. Relative motion of detectors to each other and to the field stop was unable to correct this effect. It is presumed, but not proven, that this effect is related to the high incidence angles of rays impinging on the aplanat lens and on the detector. FM2 has a detector with an improved anti-reflective coating that should have captured more of the off-axis rays. Unfortunately, this unit showed no greater field size or uniformity than the previous units. The problem may be related to the aplanat lens, which also has high incidence angle rays. An improved aplanat is planned for FM3.(2)

Special tests of out-of-field radiant response were made on the PFM and FM1 units. The latest tests were made with the instrument fully assembled. In this condition, there appears to be no influence from radiation outside the 1.8° field.

2.6 Radiometric Performance

The radiometric performance of the three instruments completed to date has been quite similar in that all units have been affected by background source variations. Each unit has shown an increase in the noise equivalent spectral radiance (NEΔN) from this source. The result is, therefore, somewhat unpredictable in that the effect of a vibration test can cause increases in the noise level. FM1 and FM2 show less tendency to change, partly because of changes made in the critical areas of the relay optics (see Section 1.4).

Radiometric response (slope) is the system response to an input and is set by the transmission characteristics of the optics, filter, and detector. The variation in filters and optics is generally not great, but the responsivity of the longwave detector differs from unit to unit, both in its peak responsivity value and the characteristics with spectral input. Shortwave detectors are more consistent, but the filters have a much greater range of transmittance than the longwave filters for a given channel. Table 2-5 lists the slope, noise, and noise-equivalent radiance for each instrument tested in the laboratory. The variation in slope and noise values are apparent from this list. The data shown in the table is taken from the final calibration in thermal vacuum tests.

The radiometric performance of the PFM and FM1 units in orbit have shown many of the tendencies observed during system test. On TIROS-N the protoflight unit did not achieve patch control temperature by approximately one degree.

(2)The tests completed to date on FM3 tend to verify that the aplanat was improved, as shown by the excellent uniformity of the longwave field.

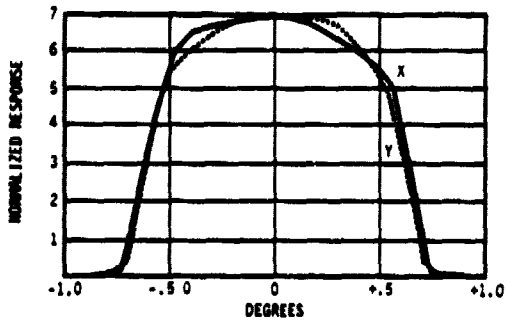

FOV CROSS SECTION, PFM, CHANNEL 8

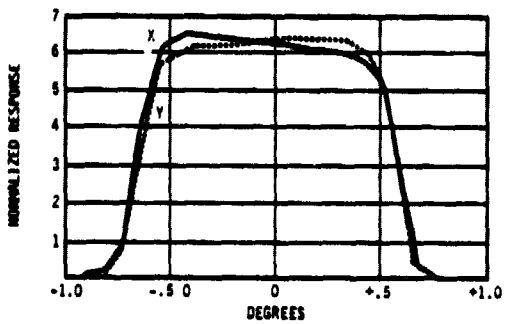

FOV CROSS SECTION, PFM, CHANNEL 19

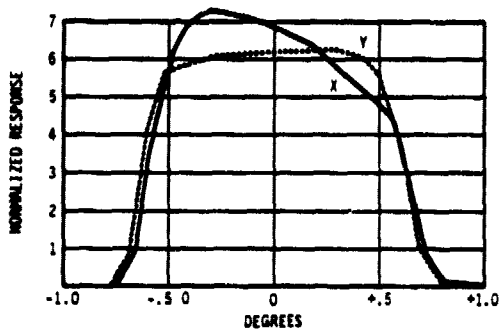

FOV CROSS SECTION, FM1, CHANNEL 8

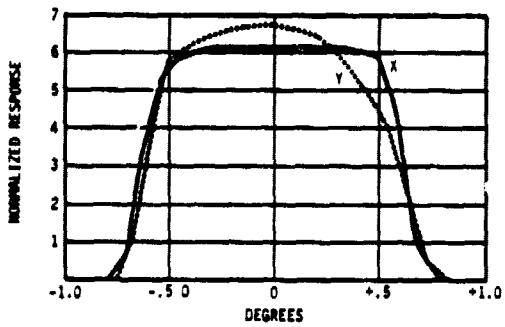

FOV CROSS SECTION, FM1, CHANNEL 19

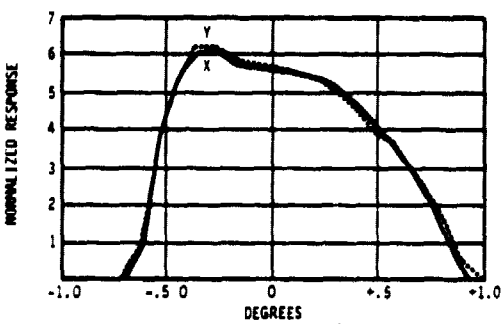

FOV CROSS SECTION, FM2, CHANNEL 8

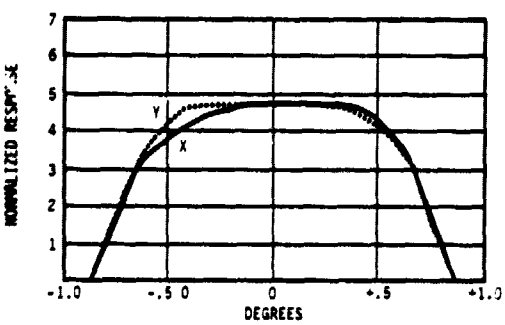

FOV CROSS SECTION, FM2, CHANNEL 19

Figure 2-3. Characteristics Of Typical Longwave And Shortwave Channels

Table 2-5. Radiometric Performance

CH	PROTOFLIGHT			FLIGHT ONE			FLIGHT TWO		
	SLOPE	σ	NEΔN	SLOPE	σ	NEΔN	SLOPE	σ	NEΔN
1	.524	4.9	2.56	.295	8.4	2.47	.497	6.4	3.18
2	.257	1.8	.46	.179	3.5	.63	.254	2.4	.61
3	.197	2.7	.53	.153	3.2	.49	.194	2.2	.43
4	.142	2.1	.30	.117	2.9	.34	.115	2.4	.28
5	.098	2.0	.19	.0807	3.9	.31	.0814	2.3	.19
6	.1055	2.3	.24	.0893	3.9	.35	.0844	2.3	.19
7	.0754	1.9	.14	.0577	3.4	.20	.0530	2.6	.14
8	.0575	1.0	.058	.0340	2.0	.068	.0424	1.0	.042
9	.0502	1.7	.030	.0408	2.0	.082	.0550	1.0	.055
10	.0610	2.5	.15	.0625	2.6	.16	.0658	1.0	.066
11	.0722	1.9	.14	.0739	2.9	.21	.0548	2.6	.14
12	.0514	3.7	.19	.0495	3.4	.17	.0411	2.3	.095
13	.00260	2.2	.0057	.00171	1.0	.0032	.00222	1.3	.0029
14	.00142	2.2	.0031	.00196	2.0	.0039	.00242	1.3	.0031
15	.00150	2.2	.0033	.00228	2.0	.0045	.00246	1.5	.0037
16	.000819	1.8	.0018	.00137	2.0	.0027	.00189	1.3	.0025
17	.000979	2.1	.0021	.00154	1.7	.0026	.00250	1.4	.0035
18	.000875	2.7	.0024	.00072	1.7	.0012	.00088	1.2	.0011
19	.000578	1.2	.0007	.00048	1.3	.00062	.00055	1.0	.00055

NOTE: o Slope is mW/m^2-SR-cm^{-1} per count. Noise is 1 σ counts from 5600 samples each channel.

o Data taken from calibration tests at ITT.

This can be seen to affect the responsivity of the detector as shown by the slope of the longwave channels.

The PFM also experienced a higher noise level in orbit than it showed in final system test for many of the longwave channels. This was not unexpected because we had seen similar increases after vibration tests. The resulting NEΔN values as shown in Table 2-6 are seen to be above the test values of Table 2-5. These values have remained essentially constant after more than nine months in orbit. The variation of patch temperature with sun angle (107.15K to 108.15K) has had only a small effect on the NEΔN (approximately five percent). There is no sign of a change in shortwave channel slopes that would indicate a reduction of optical transmission. The shortwave is a better measure of optical contamination because it does not fluctuate with patch temperature. From this experience, we can anticipate continued successful operation.

2.7 Visible Channel Performance

The visible channel is a single channel at 0.69 μm with a wide spectral bandpass. The registration of the visible channel is controlled by the shortwave field stop, providing close registration to those channels. The signal amplification uses some of the shortwave amplifier and is partly dependent on the gain of the shortwave system. Noise levels in the visible channel are very low, generally averaging about 0.4 counts standard deviation. The dynamic range for full darkness to 100 percent albedo is typically about 3500 counts, providing a very wide brightness range. The albedo in percent is calculated from the count value and an offset value.

$$Y = Ax + B$$

where Y is albedo in percent, A is multiplier for each instrument, and B is constant offset for each instrument.

	A	B
PFM	.0221	80.0
FM1	.0297	108.0
FM2	.0307	111.2

Table 2-6. Orbital Performance

	PFM, TIROS-N		FM1, NOAA-6			
	ORBIT NO CONTROL		ORBIT PRE-CONTROL		ORBIT POST CONTROL	
DATE	10/31/78		7/13/79		7/13/79	
PATCH TEMP	107.1		104.62		106.55K	
RAD. TEMP	177.8		176.5		176.4K	
	SLOPE	NEΔN	SLOPE	NEΔN	SLOPE	NEΔN
CH 1	.577	4.2	.2518	1.765	.2853	1.92
2	.272	.76	.1547	.468	.1747	.506
3	.209	.61	.1330	.379	.1497	.413
4	.150	.43	.1021	.286	.1146	.311
5	.104	.31	.0707	.237	.0793	.261
6	.111	.30	.0784	.283	.0877	.295
7	.79	.23	.5084	.164	.5676	.174
8	.61	.076	.3019	.059	.3338	.062
9	.53	.068	.3660	.068	.4040	.071
10	.66	.094	.5621	.126	.6191	.137
11	.76	.20	.6546	.179	.3212	.191
12	.53	.14	.4488	.143	.4944	.150
13	.255	.0053	.1710	.0022	.1711	.0025
14	.141	.0042	.1948	.00296	.1949	.0032
15	.149	.0033	.2247	.0038	.2248	.0037
16	.082	.0015	.1381	.00198	.1382	.0021
17	.098	.0020	.1524	.00183	.1525	.0019
18	.87	.0022	.7077	.00086	.7084	.0009
19	.57	.00065	.5010	.00048	.5016	.00049
FILTER WHEEL T.	303.1		294.1		294.1K	
PATCH POWER	0		0		8.7 mW	

NOTE: MOST SIGNIFICANT FIGURES ONLY LISTED FOR SLOPES.

3.0 CONCLUSIONS AND RECOMMENDATIONS

The HIRS/2 instruments developed and delivered for the TIROS-N program have met the program objectives of functional performance and reliability. The radiometric quality of the instruments meets the general performance level of the predecessor instrument on which the design and operational utilization were based. The instruments were not able to meet the increased sensitivity requirements stated for this program after a design change in signal processing was instituted to assure independence from non-uniform radiant fields. This change made the instrument more valid scientifically, but resulted in an increased susceptibility to small changes in radiant input at the detector. Many of the design changes described earlier were instituted to reduce this susceptibility. With a hurried assembly and delivery schedule, it was considered valuable to have instruments of this quality in orbital operation where atmospheric soundings could be routinely generated and the instrument quality assessed as part of the total sounding product. Evaluation of the operational system and the role of HIRS/2 will come from the user (NOAA) as time progresses.

The design of the HIRS/2 instrument included optical, radiometric, radiative, thermal, electronic, mechanical, and functional requirements. Details of each design are given in previous technical reports, periodic reports, design reviews, and special reports. The designs were validated by analysis and test and confirmed by orbit operation. Some characteristics of the system were limited by physical constraints imposed by the dependence on existing components and designs from HIRS/1 and from physical configuration limitations of the TIROS-N satellite.

The goals for optical excellence included close registration between all channels, uniform fields, identical field sizes, and maximum collection efficiency. The basic design of two highly registered field stops to set registration and uniformity should have provided the desired quality, but limitation of optic component size and apparent detector and optical coating inadequacy prevented achieving the goals. Improvement in optical coating efficiency at high incidence angles on the longwave aplanat lens, as mentioned in section 1.4.6, is likely to improve system performance in the near term. Lenses procured for following units have an improved surface and may show some gains.

Radiant cooler performance was limited in size by the spacecraft configuration and again by addition of stiffner rods to reduce detector susceptibility to vibration-induced background changes. From a planned 105K operating temperature with a 5K margin, the performance now has an operating temperature of 106.5K with about 2K margin. The unfortunate loss of cooler performance of the PFM on TIROS-N had the fortunate result of demonstrating a high degree of temperature stability for the detectors in the absence of active control. With this knowledge and the fact that system performance degrades slowly up to a detector temperature of 110K, the risk of flying an instrument with a

small margin is reduced. Another purpose for cooler margin is to provide excess for changes in sun angle and cooler degradation. After nine months in orbit, there appears to be no noticeable loss in optical transmission or cooler performance that would indicate degradation, again supporting the use of an instrument with small cooler margin.

Radiometric performance has been discussed in previous sections. From tests made during investigation of noise factors, it was found that the background detector and electronic noise levels are nearly one-third of those measured in system tests, indicating a capability for significantly improved performance. The influence of low-level vibration originating in the filter wheel motor can be detected as it affects radiant energy emitted from various components of the system. These components include the filter wheel, all optic elements and their mounts, all the mirrors and windows in the optic path between the filter wheel and the detector, and the detector and structure on which they are mounted. Experiments and modifications to the flight models show that reducing vibration of the motor, reducing temperature of any part of the optics system, reducing emissivity of lens holders and optic paths and stiffening the patch can all reduce the background noise. Operating the instrument with filter housing heat off reduces the temperature of some optical components and is effective. FM1 on NOAA-6 will be operated this way. Based on preliminary tests of FM3, the use of an aluminum lens holder (relay optics block) reduces lens and mount temperature and appears to be effective in reducing noise levels. Methods such as this are being considered to improve the system performance within the limitations of present system configuration and time constraints. These changes may reduce noise by ten to thirty percent, but, more importantly, may reduce the tendency to increase noise after vibration test or launch as the result of increased motor vibration and its transmission through the system.

Recommendations for near-term improvements that might be instituted in the following flight models (five additional units) include improved optical coatings on the longwave aplanat and continued evaluation of changes such as the use of the aluminum relay block. These modifications require no change in instrument configuration or operation. Operating with the filter housing heat off should be considered as a viable means of gaining performance; other approaches might be considered. Operating with patch control power off might be considered since a 2K lower detector temperature increases longwave response by approximately 15 percent.

Long-term consideration of basic improvements should include modifying the cooler assembly to (1) achieve a lower operating temperature and (2) to add excess cooling capacity to offset sun angle effects. The filter-wheel temperature and optic-system temperatures should be reviewed for design changes that could materially reduce the source temperature and the effect of low-level vibration. With a number of well considered changes, it is reasonable to achieve system performance levels consistently better than now obtained from these early models of the High Resolution Infrared Radiation Sounder.